GEOPHYSICAL RESEARCH LETTERS, VOL. 25, NO. 3, PAGES 233-236, FEBRUARY 1, 1998

The role of extensional instability in creating Ganymede grooved terrain: Insights from Galileo high-resolution stereo imaging

Geoffrey C. Collins, James W. Head III, and Robert T. Pappalardo
Department of Geological Sciences, Brown University, Providence, RI

Abstract. Galileo stereo images covering about 1500 km^2 of Uruk Sulcus on Ganymede have revealed two scales of ridges; (1) large-scale ridges and troughs spaced ~6 km apart, corresponding to the "grooves" seen in Voyager images, and (2) small-scale ridges spaced hundreds of meters apart superimposed on the large-scale ridges. We interpret the small-scale ridges to be the result of tilt-block normal faulting of the surface brittle layer, while the large-scale ridges may be due to necking of the brittle layer over a ductile substrate. The geometry of the tilt blocks revealed in Galileo images leads to a minimum estimation of 51% to 58% extensional strain in the area. The strain estimate, when incorporated into a model for the formation of grooved terrain by necking of a brittle layer undergoing extension, leads us to estimate a thermal gradient of ~20 K/km and a strain rate of ~10^{-14} s^{-1} during groove formation.

Introduction

The surface of Jupiter's largest satellite Ganymede is divided into ancient dark terrain and younger bright terrain [*Smith et al.*, 1979]. The bright terrain is characterized by sets of subparallel ridges and troughs, commonly called "grooves," and collectively known as "grooved terrain." The grooves have been interpreted by numerous authors to be the result of extensional tectonic activity in Ganymede's past [see *Squyres and Croft*, 1986, and references therein]. In Voyager images (~1 km/pixel) the grooves appear in high-sun images as dark and bright stripes, and in near-terminator images the topography of the grooves is revealed to be broadly U-shaped in cross-section. The relationship between the albedo stripes observed at high sun and the topography is not evident from the Voyager images. The spacing between grooves ranges from 5 to 10 km, with different areas of grooved terrain exhibiting different characteristic groove spacing [*Grimm and Squyres*, 1985]. The grooves have been interpreted to be open tension fractures or graben [*Squyres*, 1982], or structures formed as a result of extensional necking of a brittle layer over a ductile substrate [*Fink and Fletcher*, 1981]. *Herrick and Stevenson* [1990] modeled the conditions necessary for necking to occur on the surface of Ganymede and found the strain rate and thermal gradient required were implausibly large. These authors had to make assumptions about the depth of the grooves and the amount of extensional strain which created grooved terrain. Galileo high-resolution stereoscopic images of the grooved terrain allow measurement of the depth of the grooves and an estimate of the amount of extensional strain in the grooved terrain. In this paper, we describe some of the new insights gathered from the analysis of Galileo images and implications for the formation of grooves by necking.

Paper number 97GL03772.
0094-8534/98/97GL-03772$05.00

Galileo observations and structural interpretation

Images of grooved terrain at <100 m/pixel returned by the Galileo spacecraft (Figure 1a) have revealed that the broad ridges and troughs observed in Voyager images (Figure 1b) are further subdivided into smaller ridges and troughs a few hundred meters across [*Belton et al.*, 1996]. The broad bright and dark stripes apparent in the high-sun Voyager image are difficult to identify in the high-sun Galileo image due to the complex array of small grooves resolved in the Galileo data. Indeed, it is not readily apparent whether the "Voyager scale" of grooves really exists or is an artifact from mixing together many smaller grooves at low resolution. The Galileo spacecraft obtained stereo images of the area in Figure 1 on its first and second orbits, and the digital elevation model derived from these stereo images [Figure 1c; *Giese et al.*, 1997] clearly shows that the topography corresponds to the "Voyager scale" of grooves. Bright areas in the Voyager image correspond to topographically high areas in the digital elevation model, and dark areas in the Voyager image are topographically low. The Galileo stereo images show that the small-scale ridges follow the same general albedo pattern as the large-scale ridges. The darkest material is situated in the narrow troughs between the ridges, and the brighter material is exposed on the slopes and crests of the ridges [*Pappalardo et al.*, 1997]. The large-scale ridges and troughs are 6-7 km wide and display an asymmetry in the slope angles on either side of the ridges, appearing as rounded sawteeth in cross-section.

The small-scale ridges and troughs are not well represented in the digital elevation model because the resolution of the model is 200 m/pixel, too coarse to resolve most of the smaller ridges [*Giese et al.*, 1997]. However, it is observed through stereo viewing that the small-scale ridges are roughly triangular in cross-section. Adjacent ridges merge together in tapering ramps, and incipient fractures in older material show the surface of the bright terrain becoming progressively fractured, tilted, and extended as grooves are formed [*Pappalardo et al.*, 1997]. Deformation of the surface by tilt-block extensional faulting is the most plausible mechanism which fits these observations, and is thus likely to be the dominant process in the formation of these small-scale ridges [*Pappalardo et al.*, 1997].

Figure 2 is a schematic diagram of the topography and albedo variations across one "Voyager scale" groove, illustrating the small-scale grooves within it. In the topographic lows the small-scale ridges and troughs are smaller and more closely

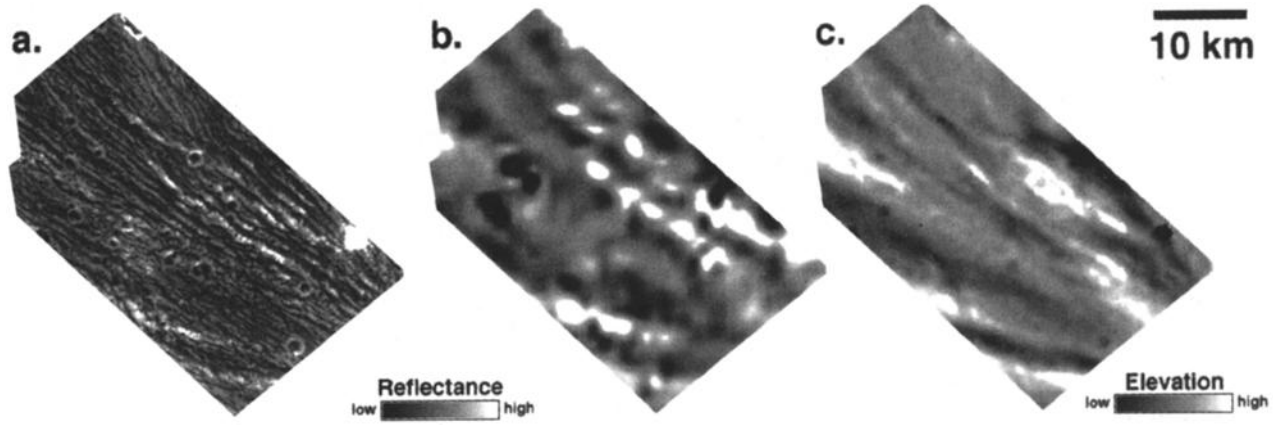

Figure 1. The Galileo Uruk Sulcus stereo target area (12°N, 169°). (a) Galileo image of the area shows pervasive sub-kilometer ridges and troughs. (b) Lower resolution Voyager data of the same area show only a few grooves at a scale of 6 km. (c) Comparison to a digital elevation model derived from Galileo stereo data [*Giese et al.*, 1997] shows that topographically low areas are characterized by darker stripes in the Voyager image and small, closely spaced ridges in the Galileo image; in contrast, topographically high areas are brighter in the Voyager image and show relatively larger ridges in the Galileo image.

spaced, as compared to the small-scale ridges and troughs situated on the topographic highs. Our structural interpretation of this surface [see also *Pappalardo et al.*, 1997] is that extension began along a detachment fault, separating the overlying brittle layer into tilt blocks. The precise nature and depth of the detachment surface is unknown; the master fault may shallow near the brittle-ductile transition, or there may be a mechanical discontinuity within the brittle layer (such as the base of possible cryovolcanic flows) which serves as a detachment. As the fault system underwent extension, necks began to form in the brittle layer, concentrating the extensional stress and thus extension strain along the faults in the necks. After continued extension, the normal faults in the necks rotated out of prime orientations and secondary normal faults may have formed [cf. *Morton and Black*, 1975]. Secondary faulting in the necks may explain the more closely spaced small-scale ridges in the topographically low areas and the greater along-strike discontinuity of these ridges as compared to the larger ridges on the topographically high areas. This secondary faulting may have been initiated as the detachment surface below the necks was bowed up by ductile flow in the substrate. As the upwarped section of the detachment became progressively unfavorable for continued shear, new master faults may have propagated to the surface of the neck to maintain the listric geometry of the detachment [*Lister and Davis*, 1989].

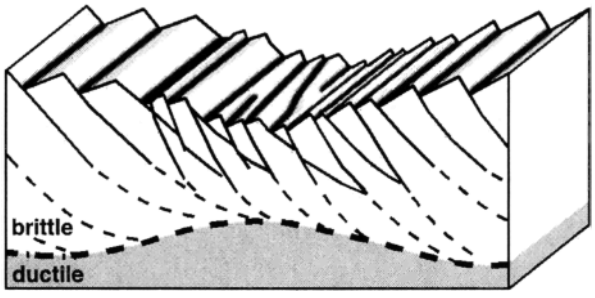

Figure 2. Schematic block diagram showing general relationships between albedo and topography of the surface within one "Voyager scale" groove in the Uruk Sulcus stereo area. Albedo variations are shown as shading and dark stripes on the surface. Solid lines in the subsurface reflect our interpretation of tilt block normal faulting, while dashed continuations of these lines are extensions of these faults to a possible detachment surface, assumed to be near the brittle-ductile transition. The brittle layer is thin and highly extended in the neck, and secondary faults have cut the primary tilt blocks in the neck to create the irregular, closely spaced ridges observed in topographic lows.

The interpretation of the small-scale ridges in the Galileo images as tilt block normal faults allows us to estimate the total amount of strain which occurred, ε. To estimate the strain, we assume a planar tilt block geometry, and that the bottoms of adjacent troughs are at the same elevation. This formulation requires an assumption of the initial fault dip θ and measurement of the projected lengths of the shorter (x) and longer (y) slopes in order to constrain the slope of the back-tilted face ϕ (figure 3):

$$\frac{y}{x} = \frac{\tan(\theta - \phi)}{\tan\phi} \quad (1)$$

The amount of strain $\varepsilon = (x+y)/s - 1$ is related to θ and ϕ by the relationship:

$$\varepsilon = \frac{\sin\theta}{\sin(\theta - \phi)} - 1 \quad (2)$$

For each tilt block along the profiles measured, the trough-to-trough distance was determined, which approximates the spacing of the faults as they presently outcrop on the surface. Then the position of the ridge crest was estimated from stereo image viewing and a correction was applied for the slight distortion due to the image emission angle. To derive a minimum strain estimate, we assumed that the longer slopes (y) represent the original surface, while the shorter slopes (x) are assumed to be the fault scarps. The ratio y/x is measured to be approximately 1.5. When this ratio and a reasonable range of initial fault dips (45°-60°) are inserted into equations (1) and (2), we calculate 51-58% extensional strain. This strain estimate is a minimum estimate because (a) the ratio y/x has been minimized by the assumption that the shorter faces of ridges are the faulted face, (b) faulting at a scale below the resolution of the images may accommodate additional extension, and (c) secondary faulting of tilt blocks in the necks may cause breakup and rotation within these blocks, masking the original geometry

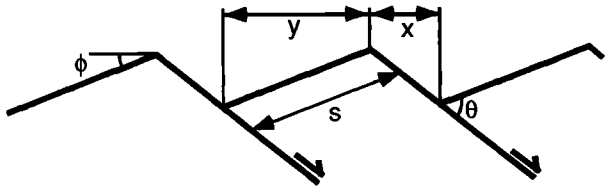

Figure 3. Geometric model of tilt-block extension along planar faults to derive an estimation of strain. The slope widths x and y are measured as viewed from directly above the surface, s is the fault spacing on the undeformed surface, θ is the initial fault dip, and ϕ is the tilt of the original surface. See equations (1) and (2).

of these tilt blocks. Also, if the faulting is occurring with a strong listric geometry, the inferred amount of strain would be reduced [*Wernicke and Burchfiel*, 1982]; however, the systematic progression of y/x across the area that would be expected from such a geometry is not observed here.

Implications for necking

Fink and Fletcher [1981] proposed that the grooves on Ganymede may result from the necking of a brittle layer of ice overlying a ductile substrate of warmer ice. Necking occurs in a brittle layer as extensional stress is concentrated in initially thin areas of the layer. Brittle materials exhibit a nonlinear relationship between stress and strain rate, so an instability may occur because positive feedback exists between a thin area of the brittle layer concentrating more stress, and the higher strain rate due to the higher stress which extends the thin area more rapidly. The ductile substrate flows to accommodate the areas of enhanced thinning in the brittle layer, and acts to suppress the topographic expression of the necking instability. Under certain conditions of strain rate and thermal gradient, a dominant wavelength of topographic variation will be amplified (see *Fletcher and Hallet* [1983] for a detailed explanation of the necking model).

Figures 4a (after *Herrick and Stevenson* [1990]) and 4b (after *Dombard and McKinnon* [1996]) show plots of temperature vs. strain rate for Ganymede, with contours of two variables. The first variable is the dominant wavelength λ of the topography being amplified, and the other is a factor q_d describing the growth of instability at the dominant wavelength. The parameter q_d is given by [*Herrick and Stevenson*, 1990]:

$$q_d = 1 + \frac{\ln(A / A_o)}{\varepsilon} \qquad (3)$$

where A is the observed topographic variation at the dominant wavelength between the ridges and troughs, A_o is the original topographic variation at this wavelength (assumed to not exceed a few meters), and ε is the total strain to which the terrain was subjected during the extensional episode.

Herrick and Stevenson [1990] modeled the possibility that grooves on Ganymede may be the result of necking. They constrained their model with estimates of the amount of extensional strain thought to have occurred over the surface of Ganymede based on Voyager images. This estimate was ≤1% based on the intact nature of Galileo Regio [*McKinnon*, 1981], and Herrick and Stevenson allowed an upper limit of 10% strain in their model to account for local concentration of strain in some areas of grooves. Estimates of the topography of the grooves based on Voyager images were on the order of a few hundred meters, so Herrick and Stevenson used a value of 100 for A/A_o (the amplification of original topography by necking). These estimates led them to conclude q_d must be greater than 40 for necking to be a viable mechanism for producing the grooves on Ganymede. They concluded that necking was not a viable model for the formation of grooves on Ganymede, because the thermal gradient and strain rate required for q_d>40 in their model are unrealistically high (cf. Figure 4a).

In their necking model, Herrick and Stevenson used the rheological parameters of ductile ice from *Kirby* et al. [1987]. Recent experiments in ice rheology designed to better simulate the low stresses and strain rates expected on icy satellites have shown that under these circumstances the deformation mechanism for ice is controlled by grain-size sensitive creep, such as grain boundary sliding [*Goldsby and Kohlstedt, 1997* and *in press*]. *Dombard and McKinnon* [1996] used this grain-size sensitive rheology, in addition to assumptions of a lower equatorial surface temperature due to lower early solar luminosity, and found that necking could occur on Ganymede at more reasonable temperature gradients and strain rates. For q_d>40, the Dombard and McKinnon model would require at least a strain

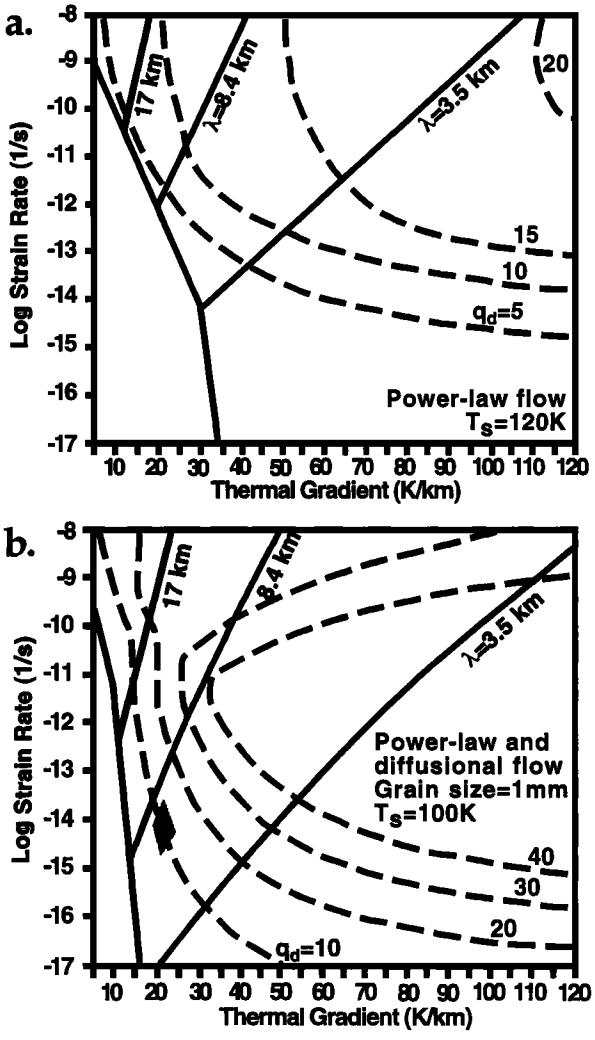

Figure 4. (a) Graph of strain rate vs. thermal gradient (after *Herrick and Stevenson* [1990]) showing contours of dominant wavelength λ and amplification factor at that wavelength q_d of the extensional instability. (b) Similar graph showing the effect of new flow law for ductile ice (after *Dombard and McKinnon* [1996]). The shaded area represents the ranges of λ and q_d estimated for the Uruk Sulcus stereo area.

rate of ~10^{-12} s^{-1} and a thermal gradient of ~40 K/km to form the grooves by necking.

Our estimate for extensional strain in the Uruk Sulcus stereo target area changes the estimate for the required value of the growth factor q_d on Ganymede for necking to be a viable process. The large-scale ridges and troughs in Uruk Sulcus show 250-500 meters of relief [*Giese et al.*, 1997], so assuming a few meters of initial topography at the dominant wavelength, we will consider a range of A/A_o values from 50-500. Strain of 51%-58% and the values of A/A_o considered yield values of q_d in the range of 8-13 from equation (3). To estimate the thermal gradient and strain rate corresponding to this range of q_d values, we use the *Dombard and McKinnon* [1996] model. The shaded area on Figure 4b represents the range of q_d values calculated above and the range of dominant wavelength (5-7 km), measured from the spacing of the necks. These ranges correspond to a temperature gradient of ~20 K/km and a strain rate of ~10^{-14} s^{-1} during groove formation, which would form the grooves in this area in a period of about 10^6 years. Inserting these values of strain rate and thermal gradient into the ductile ice flow law of *Goldsby and Kohlstedt* [1997 and in press], and finding the intersection with the frictional sliding relationship derived for ice [*Beeman et al.*, 1988], the implied thickness of the brittle layer is approximately 2 km at the time of extension.

The predictions of the necking model may become less accurate with greater amounts of strain. As strain progresses, the amplified topography at the initial dominant wavelength will be extended to longer wavelengths. Thermal re-adjustment due to thinning may not be important in Uruk Sulcus, as the timescale of conduction across the brittle layer (~10^4 years) is shorter than the timescale of the extensional episode. Also, it is unknown to what extent the brittle ice layer behaves as a plastic medium. The necking model is based on a brittle layer with slip along pervasive faults in all orientations. There may be small, pervasive faults within the brittle layer on Ganymede below the limit of image resolution which cause it to behave in a more ideal manner, but such a hypothesis is not directly testable. The asymmetry observed in the slopes of the large-scale ridges may be related to the asymmetry in the fault orientations in the tilt-block faulting model, however, modeling has not been performed to address necking of such a non-isotropic plastic medium.

Conclusion

Two scales of ridges and troughs are observed in the Galileo Uruk Sulcus stereo target area. Both of these scales may be formed during the same episode of extension. The small-scale ridges are likely to be due to brittle failure in a tilt-block normal faulting mode, while the large-scale ridges may be caused by necking of the brittle layer over a ductile substrate. The geometry of the tilt blocks indicates large amounts of extensional strain (51-58%), several times higher than estimates based on Voyager data. The increased strain estimate allows a necking instability in the grooved terrain to grow with a smaller amplification factor than previously estimated by *Herrick and Stevenson* [1990]. This results in more plausible thermal gradients (~20 K/km) and strain rates (~$10^{-14}s^{-1}$) during formation of the grooves than was previously estimated. The extensional episode which formed the grooves in the Galileo target area is likely to have occurred in a 2 km thick brittle layer and lasted on the order of 10^6 years.

It is yet to be determined whether the necking inferred for the Galileo stereo target area in Uruk Sulcus is unique to this area or common around the globe. Two scales of deformation may exist in areas of grooved terrain imaged on orbit G2. Further examination of these images is necessary to assess the extent of such phenomena. If other regions show evidence for formation by means of extensional instability, estimates can be made for the conditions of grooved terrain formation in regions outside of Uruk Sulcus.

Acknowledgments. We wish to thank B. Giese, J. Oberst, B. Schreiner, T. Roatsch, A. Cook, and G. Neukum at the DLR in Germany for their work in creating the digital terrain model from the Galileo stereo data. We also wish to thank the members of the Galileo SSI Team and the Galileo Project for making this mission a success. This work was supported by a contract from the NASA Galileo Project to JWH from the Jet Propulsion Laboratory.

References

Beeman, M., W. B. Durham, and S. H. Kirby, Friction of ice, *J. Geophys. Res.*, *93*, 7625-7633, 1988.

Belton, M. J. S., and 33 others, Galileo's first images of Jupiter and the Galilean satellites, *Science 274*, 377-385, 1996.

Dombard, A. J., and W. B. McKinnon, Formation of grooved terrain on Ganymede: Extensional instability mediated by cold, diffusional creep, *LPSC XXVII*, 317-318, 1996.

Fink, J. H., and R. C. Fletcher, A mechanical analysis of extensional instability on Ganymede, *NASA TM-84211*, 51-53, 1981.

Fletcher, R. C., and B. Hallet, Unstable extension of the lithosphere: A mechanical model for basin-and-range structure, *J. Geophys. Res.*, *88*, 7457-7466, 1983.

Giese, B., J. Oberst, B. Schreiner, T. Roatsch, A. C. Cook, G. Neukum, J. Head, and R. Pappalardo, Local topography and areal distribution of bright and dark material on Ganymede, *LPSC XXVIII*, 415-416, 1997.

Goldsby, D. L., and D. L. Kohlstedt, Flow of ice I by dislocation, grain boundary sliding, and diffusion processes, *LPSC XXVIII*, 429-430, 1997.

Goldsby, D. L., and D. L. Kohlstedt, Grain boundary sliding in fine-grained ice I, *Scr. Mater.*, in press.

Grimm, R. E., and S. W. Squyres, Spectral analysis of groove spacing on Ganymede, *J. Geophys. Res.*, *90*, 2013-2021, 1985.

Herrick, D. L., and D. J. Stevenson, Extensional and compressional instabilities in icy satellite lithospheres, *Icarus* 85, 191-204, 1990.

Kirby, S. H., W. B. Durham, M. L. Beeman, H. C. Heard, and M. A. Daley, Inelastic properties of ice I_h at low temperatures and high pressures, *J. Phys. Orsay Fr. Suppl.*, *48*, 227-232, 1987.

Lister, G. S., and G. A. Davis, The origin of metamorphic core complexes and detachment faults formed during Tertiary continental extension in the northern Colorado River region, U.S.A., *J. Struct. Geol.*, *11*, 65-94, 1989.

McKinnon, W. B., Tectonic deformation of Galileo Regio and limits to the planetary expansion of Ganymede, *LPSC XII*, 1585-1597, 1981.

Morton, W. H., and R. Black, Crustal attenuation in Afar, in *Afar Depression of Ethiopia, Inter-Union Commission on Geodynamics Scientific Report No. 14*, Verlag, 55-65, 1975.

Pappalardo, R. T., J. W. Head, G. C. Collins, and R. Greeley, The origin of grooved terrain on Ganymede: Insights from Galileo high-resolution imaging, *LPSC XXVIII*, 1063-1064, 1997.

Smith, B. A., and the Voyager Imaging Team, The Jupiter system through the eyes of Voyager 1, *Science*, *204*, 951-972, 1979.

Squyres, S. W., The evolution of tectonic features on Ganymede, *Icarus*, *52*, 545-559, 1982.

Squyres, S. W., and S. K. Croft, The tectonics of icy satellites, in *Satellites*, J. Burns and M. Matthews, eds., U. of Arizona Press, 293-341, 1986.

Wernicke, B., and B. C. Burchfiel, Modes of extensional tectonics, *J. Struct. Geol.*, *4*, 105-115, 1982.

G. C. Collins, J. W. Head, and R. T. Pappalardo, Department of Geological Sciences, Box 1846, Brown University, Providence, RI, 02912. (email: Geoffrey_Clark_Collins@brown.edu)

(Received September 5, 1997; revised November 24, 1997; accepted December 16, 1997.)